Acta Crystallographica Section A
Foundations of Crystallography
ISSN 0108-7673

Received 17 September 2003
Accepted 17 November 2003

First-principles calculations as a tool for structure validation in electron crystallography

Thomas E. Weirich

Gemeinschaftslabor für Elektronenmikroskopie der RWTH Aachen, Ahornstrasse 55, D–52074 Aachen, Germany. Correspondence e-mail: weirich@gfe.rwth-aachen.de

The crystal structures of $Ti_{11}Se_4$ [Weirich, Ramlau, Simon, Hovmöller & Zou (1996). *Nature (London)*, **382**, 144–146] and $Ti_{45}Se_{16}$ [Weirich (2001). *Acta Cryst.* A**57**, 183–191] determined previously from selected-area electron diffraction (SAED) data have been checked for their correctness by means of total energy calculations within the non-local density functional theory. The reliability of the used method was verified by test calculations carried out for the structurally related compound Ti_8Se_3, which is well known from single-crystal X-ray diffraction [Weirich, Pöttgen & Simon (1996). *Z. Kristallogr.* **212**, 929–930]. For Ti_8Se_3, structural models from both experiment and calculation show a perfect match (average agreement 0.01 Å). This proves that the geometrical optimized models from first-principles calculation can be used as a reliable alternative when good-quality X-ray results cannot be obtained. Calculations carried out for the two structures determined from electron crystallography yielded average improvement of the atomic coordinates of 0.04 and 0.09 Å for $Ti_{11}Se_4$ and $Ti_{45}Se_{16}$, respectively. The optimized cell parameters of the monoclinic structures (both space group $C2/m$, No. 12) are a = 25.51, b = 3.43, c = 19.19 Å, β = 117.9° for $Ti_{11}Se_4$ and a = 36.31, b = 3.45, c = 16.59 Å, β = 92.1° for $Ti_{45}Se_{16}$. These results prove that crystals that are too small for single-crystal X-ray diffraction and are difficult to solve by powder diffraction may nevertheless be amenable to accurate structure determination by electron diffraction structure analysis using data from standard SAED and the assumption of quasi-kinematical scattering. Moreover, this study shows that geometry optimization by first-principles calculations is the perfect tool for validation and improvement of complex structural models, which are suspected to have errors owing to the poor quality of experimental data.

1. Introduction

Electron crystallography has gained increasing attraction during the last decade since it allows determination of the atomic structure of extremely small crystallites, often only a few tens of nanometres in size (for the current status of electron crystallography, see Dorset & Gilmore, 2003). Besides several experimental obstacles in solving and refining a structure from electron-microscopy data, the final step – the validation of the obtained result – is a difficult matter in general (Spek, 2003). The low-R-factor criterion, which is commonly used in X-ray crystallography to indicate the correctness of a structure, can usually not be applied owing to the non-kinematical nature and/or poor quality of the electron data. To solve this dilemma, energy minimization and geometrical optimization by first-principles calculations within the density functional theory were recently used to verify the structure of β-Ti_2Se, which was only accessible by electron diffraction (Weirich *et al.*, 2000; Weirich & Albe, 2001; Albe & Weirich, 2003). The success of this approach has prompted the present author to check the even more complex structures of $Ti_{45}Se_{16}$ (Weirich, 2001) and $Ti_{11}Se_4$ (Weirich, Ramlau *et al.*, 1996), which could also only be determined using electron crystallography methods. Contrary to the (orthorhombic) structure of β-Ti_2Se, the latter two structures belong to the monoclinic system. Hence a reference calculation was carried out for the structurally related compound Ti_8Se_3 (Weirich *et al.*, 1996), in order to allow an estimate of how accurately such complex structures could be reproduced by quantum-mechanical calculations.

2. Method

The density functional theory (DFT) has recently become a standard for *ab initio* computer calculations in solid-state materials research and crystallography (Milman & Winkler, 1999; Winkler, 1999). Such calculations have been employed

Table 1
Lattice constants for the three investigated compounds as obtained from experiment and from total energy calculations within non-local density functional theory (DFT).

	a (Å)	*b* (Å)	*c* (Å)	*β* (°)
Ti_8Se_3 (*C*2/*m*, No. 12)				
X-ray (single crystal)	25.562 (4)	3.4411 (5)	19.701 (6)	122.25 (1)
DFT	25.56	3.44	19.70	122.7
$Ti_{11}Se_4$ (*C*2/*m*, No. 12)				
X-ray (powder)	25.516 (11)	3.4481 (14)	19.201 (6)	117.84 (3)
DFT	25.51	3.43	19.19	117.9
$Ti_{45}Se_{16}$ (*C*2/*m*, No. 12)				
SAED (single crystal)	36.53	3.45	16.98	91.7
DFT	36.31	3.45	16.59	92.1

for example to optimize rough structure models (Le Page *et al.*, 2002), to obtain an improved initial model for Rietveld refinement from an intelligent guess (Song *et al.*, 2002) or to complete structural fragments and refine H-atom positions (Kaduk, 2002). At present, there exist several codes for parameter-free DFT calculations employing pseudopotentials and plane waves.[1] The main programs used for such calculations are the Cambridge Serial Total Energy Package, *CASTEP* (Payne *et al.*, 1992; Milman *et al.*, 2000) and the Vienna *Ab initio* Simulation Package, *VASP* (Kresse & Furthmüller, 1996). Other programs have been developed more recently, *e.g. ABINIT* (Gonze *et al.*, 2002). As an alternative to a plane-wave basis with pseudopotentials, it is also possible to use localized atomic basis sets instead. This approach was originally developed for small systems like molecules and clusters and was later modified to work also for periodic structures (Delley, 2000). Nevertheless, all results presented in the following were obtained with the program *CASTEP* (Materials Studio, Accelrys Inc., San Diego, CA, USA) running on a 1.8 GHz PC equipped with 1 Gbyte RAM.

The calculations for the three structures investigated here were carried out for space-group symmetry *C*2/*m* (No. 12) with non-relativistic ultra-soft pseudopotentials (Lee, 1991) and the general-gradient approximation (GGA) to include exchange and correlation (Perdew & Wang, 1992). Unit-cell and internal coordinates were optimized by applying a BFGS[2] scheme (Fischer & Almlöf, 1992).

3. Results

3.1. Ti_8Se_3

Lattice parameters and refined atomic positions from an earlier single-crystal X-ray study on this compound (Weirich, Pöttgen & Simon, 1996) were used as input for the calculation. The kinetic energy cut-off for plane waves was set to 350 eV for this run, *i.e.* only basis functions with kinetic energy below this value are included in the basis set. The calculation was interrupted after 33 iterations (one and a half months), when the energy change was less than 1×10^{-6} eV per atom. The r.m.s. displacement[3] for the 16 titanium and 6 selenium atoms in the asymmetric unit was practically zero (1×10^{-6} Å) and the r.m.s. force less than 0.026 eV Å^{-1} at this level. The calculated lattice parameters for Ti_8Se_3 together with the corresponding X-ray data are given in Table 1. The atomic coordinates after geometrical optimization are listed in Table 2. Comparison of the result from first-principles calculation and single-crystal X-ray diffraction show an excellent match in both lattice parameters and atomic coordinates. The lattice constants *a*, *b* and *c* agree up to the second fractional digit and the monoclinic angle differs by less than 0.5°. The agreement of the two models in terms of atom coordinates is on average 0.01 Å (maximum deviation less than 0.04 Å for Ti9). The corresponding structure model obtained from first-principles calculation is shown in Fig. 1.

Table 2
Atomic coordinates for Ti_8Se_3 (space group *C*2/*m*, No. 12) as obtained from total energy calculations with the program *CASTEP* (see text).

All atoms are located on $y = 0$ (Wyckoff position 4*i*). The distance *d* gives the deviation in ångström units between the present structure model from *CASTEP* and the previously determined single-crystal X-ray structure (Weirich, Pöttgen & Simon, 1996).

	x	*z*	*d* (Å)
Ti1	0.0468	0.7180	0.01
Ti2	0.0660	0.0543	0.01
Ti3	0.0752	0.5680	0.01
Ti4	0.0951	0.4135	0.01
Ti5	0.1682	0.3404	0.02
Ti6	0.1968	0.7530	0.01
Ti7	0.2086	0.1291	0.02
Ti8	0.2240	0.6042	0.01
Ti9	0.2975	0.5357	0.04
Ti10	0.3338	0.1541	0.02
Ti11	0.4892	0.0840	0.01
Ti12	0.5121	0.4260	0.01
Ti13	0.5611	0.2856	0.01
Ti14	0.6511	0.1974	0.01
Ti15	0.7376	0.0426	0.02
Ti16	0.8733	0.0668	0.01
Se1	0.0701	0.1907	0.01
Se2	0.2421	0.2807	0.0
Se3	0.3675	0.4691	0.01
Se4	0.3930	0.3162	0.01
Se5	0.4449	0.1757	0.01
Se6	0.6304	0.0349	0.01

3.2. $Ti_{11}Se_4$

The starting point for the calculation was lattice parameters from X-ray powder diffraction and atomic coordinates obtained from electron crystallography, *i.e.* structure solution from a single high-resolution electron-microscopy image with subsequent kinematical structure refinement against intensities from SAED (Weirich, Ramlau *et al.*, 1996). The structure optimization (cut-off energy 350 eV) was stopped after 27

[1] The ionic potentials of the atoms are replaced by pseudopotentials, which are effective potentials that act only on the valence electrons of the system.
[2] A standard algorithm for solving an optimization problem developed by Broyden, Fletcher, Goldfarb & Shanno in 1970.
[3] The root mean square, r.m.s., displacement is a measure of the atom shifts that were necessary in the previous iteration step in order to decrease the total energy of the system

Table 3
Atomic coordinates for $Ti_{11}Se_4$ (space group $C2/m$, No. 12) as obtained from total energy calculations with the program *CASTEP* (see text).

The distance d gives the deviation in ångström units between the present structure model from *CASTEP* and the previous kinematical refinement with electron data (Weirich, Ramlau *et al.*, 1996).

	x	y	z	d (Å)
Ti1	0.0	0.0	0.0	0.0
Ti2	0.0837	0.0	0.9375	0.05
Ti3	0.2109	0.0	0.9295	0.03
Ti4	0.3009	0.5	0.8996	0.04
Ti5	0.4026	0.0	0.9346	0.03
Ti6	0.4872	0.0	0.8740	0.03
Ti7	0.0986	0.5	0.8349	0.05
Ti8	0.3817	0.5	0.7999	0.10
Ti9	0.4974	0.5	0.7528	0.01
Ti10	0.1177	0.0	0.7120	0.0
Ti11	0.2219	0.5	0.7070	0.02
Ti12	0.2893	0.0	0.6546	0.02
Ti13	0.3558	0.5	0.6036	0.09
Ti14	0.1599	0.0	0.5820	0.04
Ti15	0.0674	0.5	0.5708	0.01
Ti16	0.4761	0.5	0.5682	0.01
Ti17	0.2296	0.5	0.5345	0.13
Se1	0.1696	0.5	0.9915	0.10
Se2	0.1911	0.5	0.8159	0.05
Se3	0.3035	0.0	0.7985	0.0
Se4	0.0316	0.5	0.6803	0.04
Se5	0.4106	0.0	0.7187	0.09
Se6	0.3911	0.0	0.5320	0.07

iterations, which took about three months computing time. The energy change was less than 5×10^{-5} eV per atom, the r.m.s. displacement for the 17 titanium and 6 selenium atoms in the asymmetric unit was 0.022 Å and the r.m.s. force less than 0.023 eV Å^{-1} at this stage. Lattice parameters and atomic coordinates obtained from calculation are listed in Table 1 and Table 3, respectively. Comparison of lattice parameters from X-ray powder diffraction and DFT calculation show agreement for the two long axes within 0.05% whereas the short b axis deviates by 0.6%. The monoclinic angle of the two models agrees within less than 0.1°. The atomic coordinates of the two models differ on average by 0.04 Å (maximum difference 0.13 Å for Ti17). Fig. 2 shows the optimized structure model of $Ti_{11}Se_4$ in projection along its prominent short crystal axis.

3.3. $Ti_{45}Se_{16}$

Crystallographic data for the initial structure model were taken from a recent electron crystallographic study on this material, *i.e.* structure solution *via* direct methods with intensities from selected-area electron diffraction and subsequent kinematical structure refinement using the same data (Weirich, 2001). The calculations (cut-off energy 310 eV) were stopped after 46 iterations (six months), when the energy change was less than 5×10^{-5} eV per atom. The r.m.s. displacement for the 23 titanium and 8 selenium atoms in the asymmetric unit was less than 0.006 Å and the r.m.s. force less than 0.04 eV Å^{-1} at the last cycle. The calculated lattice parameters are shown in Table 1, the optimized atomic coordinates are compiled in Table 4. Analysis of the result shows a rather large deviation for the c axis of 2.4%, whereas the a axis

Table 4
Atomic coordinates for $Ti_{45}Se_{16}$ (space group $C2/m$, No. 12) as obtained from total energy calculations with the program *CASTEP* (see text).

The distance d gives the deviation in ångström units between the present structure model from *CASTEP* and the previous kinematical refinement with electron data (Weirich, 2001).

	x	y	z	d (Å)
Ti1	0.0	0	0.5	0.0
Ti2	0.0286	0.5	0.3681	0.05
Ti3	0.9401	0.5	0.4388	0.09
Ti4	0.9122	0	0.5497	0.11
Ti5	0.8961	0	0.3328	0.14
Ti6	0.8549	0.5	0.4694	0.06
Ti7	0.8780	0.5	0.6662	0.09
Ti8	0.7727	0.5	0.3391	0.10
Ti9	0.7884	0.5	0.6136	0.19
Ti10	0.7791	0	0.4819	0.12
Ti11	0.9475	0.5	0.2457	0.09
Ti12	0.0681	0.5	0.1686	0.17
Ti13	0.9788	0.5	0.0920	0.04
Ti14	0.0079	0	0.2053	0.05
Ti15	0.9110	0	0.1219	0.13
Ti16	0.9635	0	0.9533	0.05
Ti17	0.8196	0	0.2027	0.02
Ti18	0.8429	0.5	0.0625	0.12
Ti19	0.8018	0.5	0.8985	0.11
Ti20	0.7804	0	0.0132	0.20
Ti21	0.8679	0	0.9295	0.11
Ti22	0.7379	0	0.8635	0.13
Ti23	0.8134	0	0.7467	0.03
Se1	0.7596	0.5	0.7585	0.06
Se2	0.8602	0.5	0.8123	0.05
Se3	0.9126	0.5	0.0006	0.07
Se4	0.8753	0.5	0.2122	0.11
Se5	0.8269	0	0.3623	0.01
Se6	0.8395	0	0.5841	0.02
Se7	0.9730	0	0.3495	0.02
Se8	0.0706	0	0.2918	0.12

agrees by 0.6% and the short b axis was perfectly reproduced by calculation. The monoclinic angle differs by only 0.4°. The agreement of the two models in terms of atom coordinates is on average better than 0.09 Å (maximum deviation 0.20 Å for Ti20). Fig. 3 shows the optimized structure model of $Ti_{45}Se_{16}$ in projection along its prominent short crystal axis.

4. Discussion

The idea of improving poor-quality structure models with the help of computer power is in general not a new one. Attempts were made by Waser (1963), Smith & Arnott (1978), Meier & Villinger (1969) and Baerlocher *et al.* (1978). These approaches are mainly based on constraints like predefined distances and angles between atoms, which are imposed during optimization in order to find the structure with the best geometry. These approaches have been successfully applied to the refinement of less ordered polynucleotides, polysaccharides and other fibrous materials (Smith & Arnott, 1978) and for structural characterization of framework silicates (Baerlocher *et al.*, 1978). In order to work properly, all these approaches require that the interatomic distances/angles of the investigated system are well known (see Bergerhoff & Brandenburg, 1999; Allen *et al.*, 1999). Other approaches to cope with this

problem, in particular for solving crystal structures, make extensive use of empirical potential functions (Putz *et al.*, 1999) or solid-state force-field calculations to validate the proposed structural model (Engel *et al.*, 1999). However, whereas organic, and also many inorganic, materials often fit well into one of the above-mentioned schemes (the carbon—carbon distance for example is practically a constant), metallic systems are much more flexible and interatomic distances can vary over a much wider range. For this reason, first-principles calculations, which do not rely on empirical or fixed parameters, are best suited to geometrical optimization of such systems (see Milman *et al.*, 2000). The price to pay, however, is the enormous computing times that are needed to optimize larger structures.

Nevertheless, in an earlier study (Albe & Weirich, 2003) on the orthorhombic structure of α-Ti_2Se, it was shown that *CASTEP* geometrical optimization yields an identical structure model to that obtained by single-crystal X-ray diffraction. Lattice parameters were in agreement within 0.1% and the six titanium and three selenium atoms per asymmetric unit differed on average by only 0.02 Å in position (maximum deviation 0.04 Å). Thus, the geometrical optimized structure model obtained from first-principles calculations was considered as a reliable reference model for structure validation in cases where no or only incomplete structural data exist. Using this argument, it was then possible to confirm the structure of β-Ti_2Se, which was only accessible by electron diffraction structure analysis. Despite this promising result, it remained unclear if this approach would work as successfully for more complex structures, in particular for structures with variable cell angles. Nonetheless, the result obtained for Ti_8Se_3 demonstrates the reliability of this approach for such cases. The lattice constants for this test structure agree up to the second fractional digit and the monoclinic angle differs by less than 0.5°. The corresponding atomic coordinates for Ti_8Se_3 agree on average by 0.01 Å (maximum deviation less than 0.04 Å). With this proof of reliability for complex monoclinic titanium–selenium structures, it is possible to judge the quality of the other two structures for which no structural models from X-ray diffraction exist.

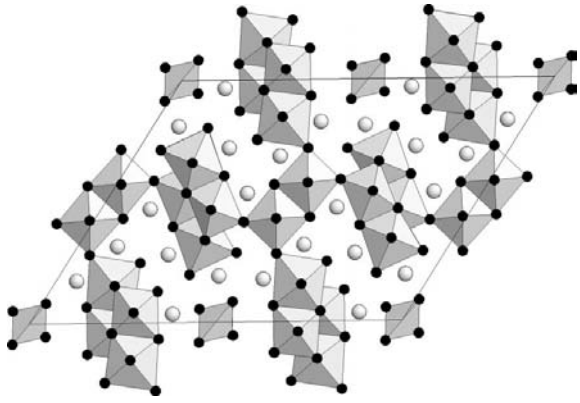

Figure 1
Structure model of Ti_8Se_3 in projection along the short *b* axis. The model represents the geometrical optimized structure as obtained from total energy calculations with the program *CASTEP* (see text). Comparison with the structures shown in Figs. 2 and 3 shows the common feature of distorted corner- and edge-sharing (condensed) octahedral Ti_6 cluster units. The Se atoms are located inside the almost regular trigonal prisms of titanium (Ti = dark circles, Se = light circles).

The compound $Ti_{11}Se_4$ was first identified as one component in a biphasic powder sample obtained from high-temperature synthesis. Owing to the absence of large single crystals, the structure was solved from high-resolution electron-microscopy images *via* crystallographic image processing. A subsequent (kinematical) refinement using a data set of *h*0*l* SAED intensities that were estimated from an exposure series on film yielded an *R* factor of 14.7%. Improved lattice parameters were later derived from the indexed peak positions in the X-ray powder diagram (Weirich, Ramlau *et al.*, 1996). A recently undertaken reinvestigation of the sample with the aim to refine the earlier determined atom positions by Rietveld analysis of the X-ray powder pattern failed owing to the presence of impurities and the complexity of the structure.

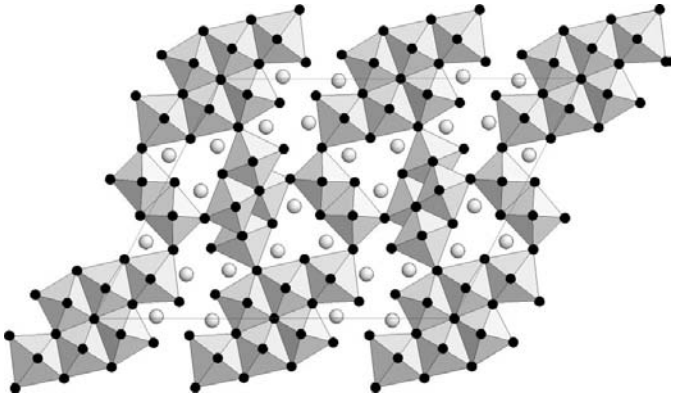

Figure 2
Structure model of $Ti_{11}Se_4$ in projection along the short *b* axis. The model represents the geometrical optimized structure as obtained from total energy calculations with the program *CASTEP* (see text). Ti = dark circles, Se = light circles

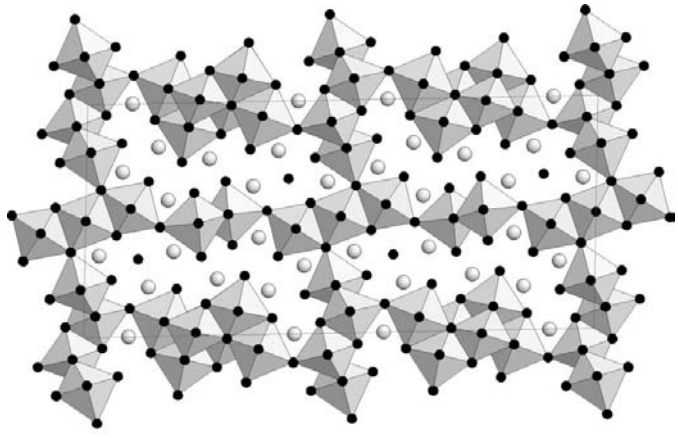

Figure 3
Structure model of $Ti_{45}Se_{16}$ in projection along the short *b* axis. The model represents the geometrical optimized structure as obtained from total energy calculations with the program *CASTEP* (see text). Ti = dark circles, Se = light circles

However, the results obtained in this study from geometrical optimization asserted the correctness of the earlier determined structure. The lattice parameters could be reproduced within 0.6% for the short axis and within 0.05% for the two long crystal axes. Notably, the monoclinic angle of the experimental and calculated model differs by just 0.1°. The atomic coordinates agree on average within 0.04 Å (maximum difference 0.13 Å). The observed small differences between the two models may originate from errors in estimating the intensities from film, influences of dynamical and secondary scattering on the intensities (see Weirich, 2003) and a small error since only projected data have been used in the refinement (see Vainshtein, 1964, p. 282*ff*.).

Analogous to the latter compound, $Ti_{45}Se_{16}$ was first discovered by electron microscopy as one component in a polyphasic powder sample. Again, a rough structure model of the compound was derived from high-resolution electron-microscopy images (Weirich, 1996). In a later study, the structure was independently solved and (kinematically) refined (*R* factor 33%) using *h*0*l* SAED intensities estimated from a typical diffraction pattern recorded on EM film (Weirich, 2001). The result obtained in this study shows that the earlier published structural parameters from electron diffraction are very close to the geometrical optimized model. The striking discrepancies of some lattice parameters (*c* axis 2.4%, *a* axis 0.6%) are probably caused by a slight misalignment of the crystal from the ideal (eucentric) specimen height and by small crystal tilt (*a* axis = tilt axis), which was detected during closer inspection of the negative. Owing to the presence of several phases in the sample, X-ray powder data could not be employed in this case to get more accurate cell parameters for comparison. However, the monoclinic angle determined from the electron diffraction pattern deviates by just 0.4° from the calculation. Since only a single electron diffraction pattern was used to estimate intensities (for the method, see Zou *et al.*, 1993*a*,*b*), the average deviation between experimental and calculated atomic coordinates is accordingly much larger than for $Ti_{11}Se_4$, where a more precise data set from an exposure series on film was used. Thus, slight misplacements of atoms in the original model of $Ti_{45}Se_{16}$ can be attributed to errors in the estimated intensities and to contributions by dynamical diffraction and/or secondary scattering. Misplacements of atoms of the same order were also found for much less complicated structures, such as α-Ti_2Se and Zr_2Se, which have been determined using the same approach as described for $Ti_{45}Se_{16}$ (Albe & Weirich, 2003; Weirich, 2003, 2004). However, despite the rather poor quality of the data for $Ti_{45}Se_{16}$ (*R* factor after LS refinement 33%), the experimental model is surprisingly close to the optimized model from calculation which can be explained using Sayre's theorem (see Weirich, 2001, 2003).

All metal-rich compounds investigated here contain octahedral Ti_6 cluster units, which can be regarded as fragments of the body-centered cubic (b.c.c.) metal itself (Fig. 4*a*). As pointed out by Simon (1981), these units may form larger regions by condensation *via* common corners, edges or faces as outlined in Figs. 1, 2 and 3. Whereas the metal-rich regions are obviously rather flexible and tolerate distortions, the trigonal prisms around the Se atoms appear almost perfectly regular [see for comparison the ideal polyhedra in Figs. 4(*b*) to (*d*)]. This suggests that the energy gain that goes along with formation of quasiregular trigonal prisms is likely to be one of the driving forces that stabilizes these metal-rich structures. The trend to favor formation of almost perfect trigonal prisms is also seen in the plots of the nearest Ti—Se distances (Fig. 5), which shows a large number of Ti—Se distances in the narrow range between 2.58 and 2.66 Å for the three structures.

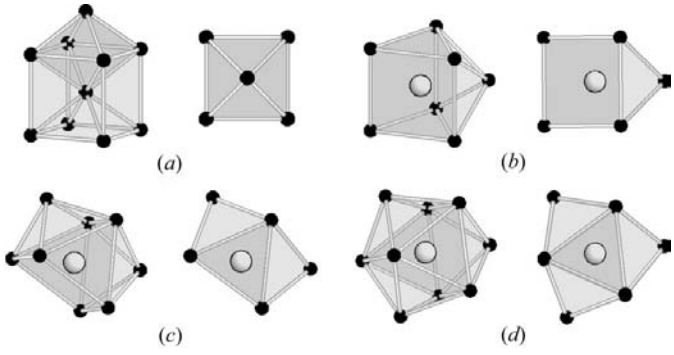

Figure 4
Types of polyhedra that build up the structures of Ti_8Se_3, $Ti_{11}Se_4$ and $Ti_{45}Se_{16}$. Each polyhedron is shown in clinographic view (left) and as observed when the structure is projected along the short crystal axis (right view). Titanium atoms are shown in black, selenium atoms in light grey. (*a*) Cube of body-centered β-titanium as vertex linked (condensed) Ti_6 octahedron; (*b*) single-capped trigonal prism with selenium at the center; (*c*) double-capped trigonal prism; (*d*) triple-capped trigonal prism.

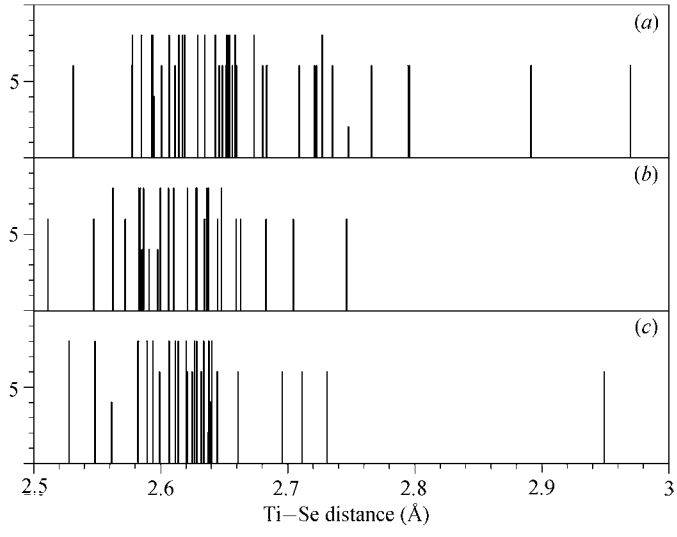

Figure 5
Calculated nearest atom distances for the geometrical optimized structures of $Ti_{45}Se_{16}$ (*a*), $Ti_{11}Se_4$ (*b*) and Ti_8Se_3 (*c*). All structures show a large number of Ti—Se distances in the range between 2.58 and 2.66 Å. These distances belong to the quasiregular trigonal prisms formed by the titanium atoms around selenium. This suggests that the energy gain that accompanies formation of trigonal prisms with optimized Ti—Se distances is probably one of the dominant driving forces that stabilizes this type of metal-rich structure.

5. Conclusions

The complex crystal structure of monoclinic Ti_8Se_3 was used to prove that structural models obtained from *ab initio* total energy calculations within density functional theory are practically identical to those obtained from standard single-crystal X-ray diffraction. The accuracy of the optimized atom positions is analogous to that from routine powder studies (Milman *et al.*, 2000; Le Page *et al.*, 2002). Total energy calculations are hence a perfect tool to check and optimize crystal structures that have been determined from poor-quality data sets. This approach is of special importance for electron crystallography, which aims at crystal structure determination of nanosized materials beyond the capabilities of conventional X-ray diffraction. The quality of standard electron diffraction data suffers frequently from misorientation of the crystal (crystal tilt) and dynamical/secondary scattering. Moreover, errors in the final structure model (misplaced atoms) may result from wrongly estimated intensities of strong reflections (film data) and in cases when only projected data are used for refinement (present case). However, these errors are totally eliminated when the structure is optimized using the method described above.

The success of the proposed approach is demonstrated on the complex metal-rich structures of $Ti_{11}Se_4$ and $Ti_{45}Se_{16}$, whose structures could only be determined from electron-microscopy data. Both of these previously unknown structures (each of them represents a structure type) are now confirmed by first-principles calculations. The calculations provide for both structures improved atomic coordinates (improvement of 0.04 and 0.09 Å, respectively) and yielded for $Ti_{45}Se_{16}$ a set of more accurate lattice constants. Thus the obtained results can be interpreted two ways:

(i) The structures were almost accurately determined despite the use of intensities determined from EM film and the crude approximation of quasikinematical scattering for refinement.[4] Thus, crystals that are too small for single-crystal X-ray diffraction and difficult to solve by powder diffraction may nevertheless be amenable to accurate structure determination by electron diffraction structure analysis from standard electron diffraction data.

(ii) Provided the geometrical optimization using first-principles calculations works reliably for a chosen system (which must be checked), only a roughly correct model – close enough to the global minimum – might be sufficient to guide the program to the structure with lowest energy. The required initial model can either be obtained from structure solution *via* direct methods with sparse electron diffraction data or from high-resolution electron-microscopy images using crystallographic image processing (Hovmöller *et al.*, 1984; Weirich *et al.*, 1997) or exit-wave reconstruction (Coene *et al.*, 1996; Zandbergen *et al.*, 1997).

[4] To the present author's knowledge, so far no method exists for structure refinement with standard SAED intensities that takes full *n*-beam dynamical diffraction into account. It should be noted that the multislice least-squares method proposed by Jansen and co-workers (Jansen *et al.*, 1998) requires data from electron microdiffraction since crystal thickness is a parameter to be refined.

The author thanks D. L. Dorset (ExxonMobil Research and Engineering Company) and M. Gemmi (University of Milan) for their valuable comments on the manuscript, and Karsten Albe (Darmstadt University of Technology) for stimulating discussions about contemporary quantum mechanics.

References

Albe, K. & Weirich, T. E. (2003). *Acta Cryst.* A**59**, 18–21.
Allen, F. H., Watson, D. G., Brammer, L., Orpen, A. G. & Taylor, R. (1999). *International Tables for Crystallography*, Vol. C, *Mathematical, Physical and Chemical Tables*, edited by A. J. C. Wilson & E. Prince, pp. 782–803. Dordrecht: Kluwer Academic Publishers.
Baerlocher, Ch., Hepp, A. & Meier, W. M. (1978). *DLS-76, a Program for the Simulation of Crystal Structures by Geometric Refinement.* Institute of Crystallography and Petrography, ETH Zürich, Switzerland.
Bergerhoff, G. & Brandenburg, K. (1999). *International Tables for Crystallography*, Vol. C, *Mathematical, Physical and Chemical Tables*, edited by A. J. C. Wilson & E. Prince, pp. 770–781. Dordrecht: Kluwer Academic Publishers.
Coene, W. M. J., Thust, A. & Op de Beeck, M. (1996). *Ultramicroscopy*, **64**, 109.
Delley, B. (2000). *J. Chem. Phys.* **113**, 7756.
Dorset, D. L. & Gilmore, C. J. (2003). *Z. Kristallogr.* Vol. 218. Special issue on Electron Crystallography.
Engel, G. E., Wilke, S., König, O., Harris, K. D. M. & Leusen, F. J. J. (1999). *J. Appl. Cryst.* **32**, 1169–1179.
Fischer, T. H. & Almlöf, J. (1992). *J. Phys. Chem.* **96**, 9768–9774.
Gonze, X., Beuken, J.-M., Caracas, R., Detraux, F., Fuchs, M., Rignanese, G.-M., Sindic, L., Verstraete, M., Zerah, G., Jollet, F., Torrent, M., Roy, A., Mikami, M., Ghosez, Ph., Raty, J.-Y. & Allan, D. C. (2002). *Comput. Mater. Sci.* **25**, 478–492.
Hovmöller, S., Sjögren, A., Farrants, G., Sundberg, M. & Marinder, B. O. (1984). *Nature (London)*, **311**, 238 – 241.
Jansen, J., Tang, D., Zandbergen, H. W. & Schenk, H. (1998). *Acta Cryst.* A**54**, 91–101.
Kaduk, J. A. (2002). *Acta Cryst.* B**58**, 370–379.
Kresse, G. & Furthmüller, J. (1996). *Phys. Rev. B*, **54**, 11169–11186.
Le Page, Y., Saxe, P. W. & Rodgers, J. R. (2002). *Acta Cryst.* B**58**, 349–357.
Lee, M. H. (1991). PhD thesis, Cambridge University, England.
Meier, W. M. & Villinger, H. (1969). *Z. Kristallogr.* **129**, 411–423.
Milman, V. & Winkler, B. (1999). *Int. J. Inorg. Mater.* **1**, 273–279.
Milman, V., Winkler, B., White, J. A., Pickard, C. J., Payne, M. C., Akhmatskaya, E. V. & Nobes, R. H. (2000). *Int. J. Quantum Chem.* **77**, 895–910.
Payne, M., Teter, M., Allen, D., Arias, T. & Joannopoulos, J. (1992). *Rev. Mod. Phys.* **64**, 1045–1097.
Perdew, J. & Wang, Y. (1992). *Phys. Rev.* B**45**, 13244–13249.
Putz, H., Schön, J. C. & Jansen, M. (1999). *J. Appl. Cryst.* **32**, 864.
Simon, A. (1981). *Angew. Chem. Int. Ed. Engl.* **20**, 1–22.
Smith, P. J. C. & Arnott, S. (1978). *Acta Cryst.* A**34**, 3–11.
Song, Y., Zavalij, P. Y., Suzuki, M. & Whittingham, M. S. (2002). *Inorg. Chem.* **41**, 5778–5786.
Spek, A. L. (2003). *J. Appl. Cryst.* **36**, 7–13.
Vainshtein, B. K. (1964). *Structure Analysis by Electron Diffraction.* Oxford: Pergamon Press.
Waser, J. (1963). *Acta Cryst.* **16**, 1091–1094.
Weirich, T. E. (1996). PhD thesis, University of Osnabrück, Germany.
Weirich, T. E. (2001). *Acta Cryst.* A**57**, 183–191.
Weirich, T. E. (2003). *Z. Kristallogr.* **218**, 269–278.
Weirich, T. E. (2004). *Crystallogr. Rep.* [Engl. transl. *Kristallografiya.*] In the press.
Weirich, T. E. & Albe, K. (2001). *Z. Kristallogr.* Suppl. 18, p. 63.
Weirich, T. E., Pöttgen, R. & Simon, A. (1996). *Z. Kristallogr.* **212**, 929–930.

Weirich, T. E., Ramlau, R., Simon, A. & Hovmöller, S. (1997). *Electron Crystallography*, edited by D. L. Dorset, S. Hovmöller & X. D. Zou, pp. 423–426. Dordrecht: Kluwer Academic Publishers.
Weirich, T. E., Ramlau, R., Simon, A., Hovmöller, S. & Zou, X. D. (1996). *Nature (London)*, **382**, 144–146.
Weirich, T. E., Zou, X. D., Ramlau, R., Simon, A., Cascarano, G. L., Giacovazzo, C. & Hovmöller, S. (2000). *Acta Cryst.* A**56**, 29–35.
Winkler, B. (1999). *Z. Kristallogr.* **214**, 506–527.
Zandbergen, H. W., Andersen, S. J. & Jansen, J. (1997). *Science*, **277**, 1221–1225.
Zou, X. D., Sukharev, Y. & Hovmöller, S. (1993*a*). *Ultramicroscopy*, **49**, 147–158.
Zou, X. D., Sukharev, Y. & Hovmöller, S. (1993*b*). *Ultramicroscopy*, **52**, 436–444.